Development of a detector based on Silicon Drift Detectors for gamma-ray spectroscopy and imaging applications

P. Busca,[a,b] **A.D. Butt,**[a,b] **C. Fiorini,**[a,b,1] **A. Marone,**[a,b] **M. Occhipinti,**[a,b] **R. Peloso,**[a,b] **R. Quaglia,**[a,b] **L. Bombelli,**[a,b] **G. Giacomini,**[c] **C. Piemonte,**[c] **F. Camera,**[b,e] **A. Giaz,**[b] **B. Million,**[b] **N. Nelms**[d] **and B. Shortt**[d]

[a] *Politecnico di Milano, Dipartimento di Elettronica, Informazione e Bioingegneria, Via Golgi 40, 20133, Milano, Italy*

[b] *Istituto Nazione di Fisica Nucleare — Sezione di Milano, Via Celoria 16, 20133, Milano, Italy*

[c] *Fondazione Bruno Kessler — FBK, Via Sommarive, 18, 38123, Trento, Italy*

[d] *European Space Agency — ESTEC, NL-2200 AG Noordwijk, The Netherlands*

[e] *Università degli studi di Milano, Dipartimento di Fisica, Via Celoria 16, 20133, Milano, Italy*

E-mail: carlo.fiorini@polimi.it

RECEIVED: *October 24, 2013*
REVISED: *November 27, 2013*
ACCEPTED: *March 16, 2014*
PUBLISHED: *May 6, 2014*

[1] Corresponding author.

1 Introduction

In this work we present first results of the development of a gamma detector based on Silicon Drift Detectors (SDDs) arrays to readout large (e.g. 1"×1" up to 3"×3") lanthanum halide scintillators, like $LaBr_3$:Ce, for gamma-ray spectroscopy and imaging measurements.

The main application is foreseen in the framework of gamma-ray astronomy observations, in a project supported by European Space Agency.[1] In this application, the elemental composition of planets could be revealed by the analysis of the major gamma-ray lines generated spontaneously by radioactive decay or by stimulated emission from Cosmic background and highly energetic particles originating from the Sun [1]. Currently, a state-of-the-art detector solution is represented by $LaBr_3$:Ce coupled to a photomultiplier tube (PMT). This detector allows to achieve a good energy resolution, but still with the limitations from the PMT in terms of low quantum efficiency, bulky structure and high voltage biasing. Moreover, PMTs demonstrate saturation and non-linear effects in the wide energy range (from 150 keV to 15 MeV) required in this application, an issue that can be addressed by reducing biasing voltage of the number of dynodes [2] or by modifying the voltage divider itself [3]. A second astrophysics application foresees the use of SDDs for the readout of scintillator crystals used in a Compton telescope gamma-ray observatory such as the GRIPS mission concept (http://www.grips-mission.eu/).

Another possible application of this detector based on $LaBr_3$:Ce and SDDs could be in nuclear physics basic research to study nuclei far from the stability line [4]. The imaging capability could

[1]Research activity supported by European Space Agency, contract number 4000102940/11/NL/NR.

in principle be exploited jointly with the spectroscopy capability in order to reduce the Doppler Broadening effect, in experiments where the gamma-ray source moves at high/relativistic velocity.[2]

The SDD is a detector characterized by a very low capacitance at the electrode collecting the signal charge, which is independent of the active area of the device. This feature guarantees low electronic noise, making it an ideal device for X-ray spectroscopy applications [5]. It is worth noting that no multiplication mechanism is used, with the benefits, on one hand, to avoid the associated statistical spread of the signal and, on the other hand, to provide higher dynamic range. Moreover, the SDD shows high quantum efficiency in the visible and near ultraviolet range, and as such are an attractive alternative to PMT readout of scintillators. State-of-the art performances have been achieved in gamma-ray spectroscopy with a single SDD coupled to small CsI:Tl [6] and $LaBr_3$:Ce scintillators [7].

As a consequence, this technology appears to also offer a convenient solution for the readout of scintillators with larger size (e.g. 1"×1" up to 3"×3") by arrays of multiple SDDs, whilst maintaining or even improving the current performance achievable with PMTs. Additional benefits of a SDD readout scheme include a more compact detection module and the avoidance of saturation in the considered energy range. Moreover, the SDD is compatible with magnetic fields.

Regarding the geometry of the scintillator, it should be noted that a thickness/diameter ratio of the crystal, near or even exceeding unity, represents a difficulty for imaging, since the correlation between light distribution and point of interaction is degraded. Halide scintillators are sold pre-packaged by the manufacturer, wrapped with reflectors on all sides, except for the optical window and sealed in an Aluminium housing with a quartz optical window. This wrapping enhances spectroscopic performance, but leads to a more challenging imaging capability, since light tends to spread quite uniformly over all photodetector units, with limited dependence upon the point of interaction of the gamma-ray interaction in the crystal volume.

In this work, we present the first results obtained with a multi-SDD photodetector array produced at Fondazione Bruno Kessler (FBK) semiconductor laboratories. The single unit of this array has already shown excellent performances when directly irradiated with X-rays and when coupled with a small $LaBr_3$ scintillator [8]. The SDD array presented here has first been irradiated with X-rays in order to estimate the electronic noise. Then, gamma-ray spectroscopy measurements, as well as linearity estimations, have been carried out by coupling the SDD array with a 1"×1" $LaBr_3$:Ce scintillator, using multiple sources in the 122–1330 keV range. The imaging capability has been evaluated by means of a collimated (1 mm diameter) Cs-137 source and operating a scan on the same scintillator with step of 5 mm along the vertical and horizontal directions. A suitably modified centroid method is finally applied to retrieve the position of interaction.

2 Detection system architecture

We are currently developing a prototype to readout large $LaBr_3$:Ce scintillators of different diameters (up to 3"×3") with the final aim to detect gamma-rays in a wide dynamic range (150 keV up to

[2]Research activity supported by Istituto Nazionale di Fisica Nucleare, within the GAMMA experiment. This work was also supported by NuPNET — ERA-NET within the NuPNET GANAS project, under grant agreement no. 1 202914 and from the European Union, within the "7thFrameworkProgram" FP7/2007-2013, under grant agreement no. 262010 — ENSAR-INDESYS.

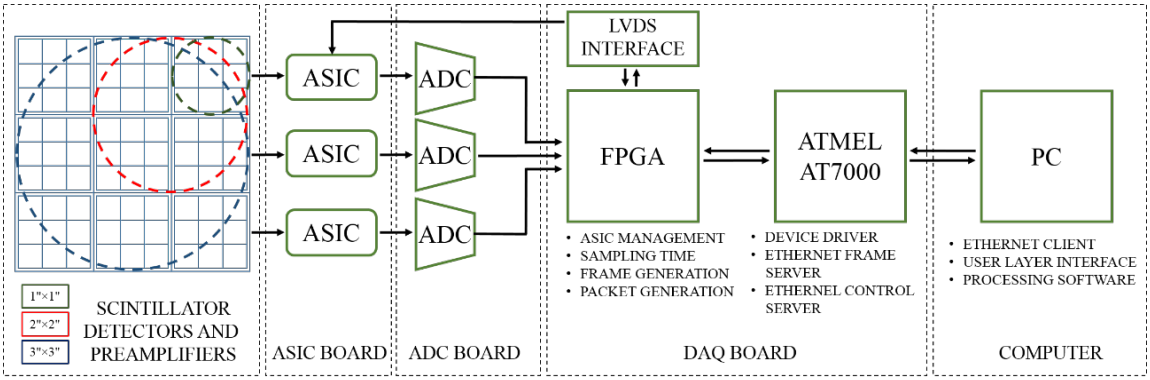

Figure 1. Block diagram of the complete readout scheme.

15 MeV), providing an energy resolution better than 3% at the 662 keV energy line. An overview of the complete architecture is shown in figure 1 . In the next sections, the SDD photodetectors employed in the system and the readout electronics are specifically described.

2.1 The Silicon Drift Detector array

The fundamental element of the detection system is a monolithic array of nine square-shaped SDDs, arranged in a 3×3 format, where each SDD has an active area of 8 mm × 8 mm, for an overall active area of 24 mm × 24 mm. The active area is surrounded by 1 mm frame of dead area for a final format of the array of 26 mm × 26 mm. The photodetector area to readout different sized scintillators is obtained by assembling a suitable number of these arrays (see figure 1), e.g. one, four and nine arrays can be coupled respectively to 1"×1", 2"×2" and 3"×3" scintillators.

The size of the single SDD unit and, accordingly, of the number of SDDs to be employed in the arrays is the result of an optimization study. Indeed, the appropriate cell size deals with both achievable energy resolution and practical requirements related to the realization of the instrument. A detailed description for the criteria adopted to optimize the cell size is provided in [8].

The SDDs array has been fabricated on NTD (Neutron Transmutation Doping), <100>, 450 μm thick wafers. NTD is commonly used for large area SDDs, since it provides a low dopant fluctuation, keeping a straight trajectory for the electrons drifting from the carrier generation point to the anode. The array has an asymmetric structure, the light entrance window, referred to as *back side*, and the collection electrode, referred to as *n-side*, are placed on the opposite sides of the wafer. The back side, shown in figure 2 (left), is realized with a uniform large junction common to all nine cells, optimized for UV light detection. This part of the light spectrum is quite critical since the photon absorption takes place within 10–20 nm from the surface. A very shallow junction is thus required to avoid recombination of the photo-generated carriers. Furthermore, a special Anti-Reflecting Coating has been developed to minimize the light reflected from the detector surface.

The anode-side is quite standard, with the same structure replicated for all nine cells. The anode is placed at the centre of the SDD with the drift p-rings with a pitch of 50 μm surrounding it. An integrated voltage divider connects each ring with its neighbours and defines a linear voltage drop from the first to the last ring (figure 2 (right). On both sides, a guard ring structure made of 10 rings is used to gradually decrease the bias voltage to ground.

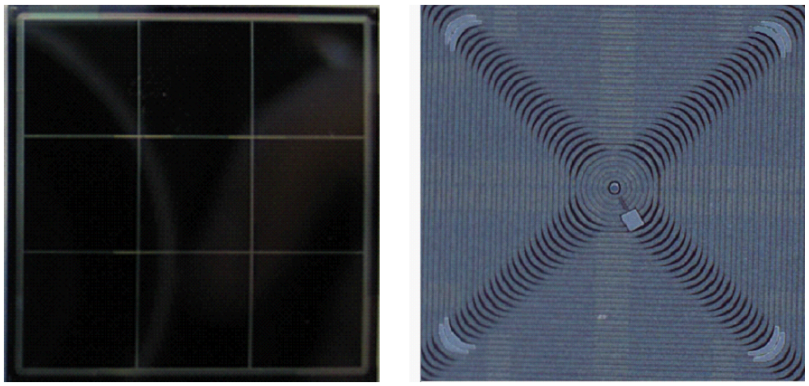

Figure 2. (left) Picture of the back the SDD, with the nine cells. (right) Detail of the n-side of one single cell.

In order to bias the electrode which acts as entrance window for the SDD without contacting it, we have adopted a technique based on punch through between the back electrode and the last drift ring in the opposite side. This technique is described in detail in [8, 9]. With this bias scheme it is possible to avoid the electrical connections on the back side of the detector, thus allowing an easy optical coupling of the array with the scintillator.

2.2 The readout electronics

The readout electronics comprise of two ASICs (Application Specific Integrated Circuits), a choice that allows handling a high number of channels within a very compact architecture with low power consumption and very good noise performance.

The first ASIC is a front-end CMOS charge preamplifier (CUBE) mounted close to the detector in order to provide low electronic noise. This preamplifier has allowed to achieve state-of-the-art noise performance using relatively standard SDD technology process and CMOS electronics [10].

The second chip has been designed in 0.35 μm (3.3V) CMOS technology [11]. This ASIC features 27 analog channels, hence up to three SDDs arrays can be readout by a single ASIC. Each channel includes a 7 complex pole semi-Gaussian shaper, a baseline holder and a peak stretcher. The relatively high order complex poles shaper amplifier is necessary to guarantee both low noise and reduced dependence to ballistic deficit with respect to more conventional CR-RC^n real-pole filters. The circuit also features a 160 bit internal register to program 4 different peaking times (2 μs, 3 μs, 4 μs and 6 μs), as well as 3 gain settings. The system also allows the setting of independent threshold levels for each channel and the possibility to ignore unused or malfunctioning channels. The ASIC digital section is composed of a 27:1 analog multiplexer connected to the output of all the channels and a differential buffer used to drive an external ADC.

Up to three ASICs boards can be hosted in a mother board with the purpose of supplying analog and digital signals to the DAQ. The DAQ board converts all data coming from the three ASICs, with a resolution of 16 bits, and is interfaced to the host PC via Ethernet.

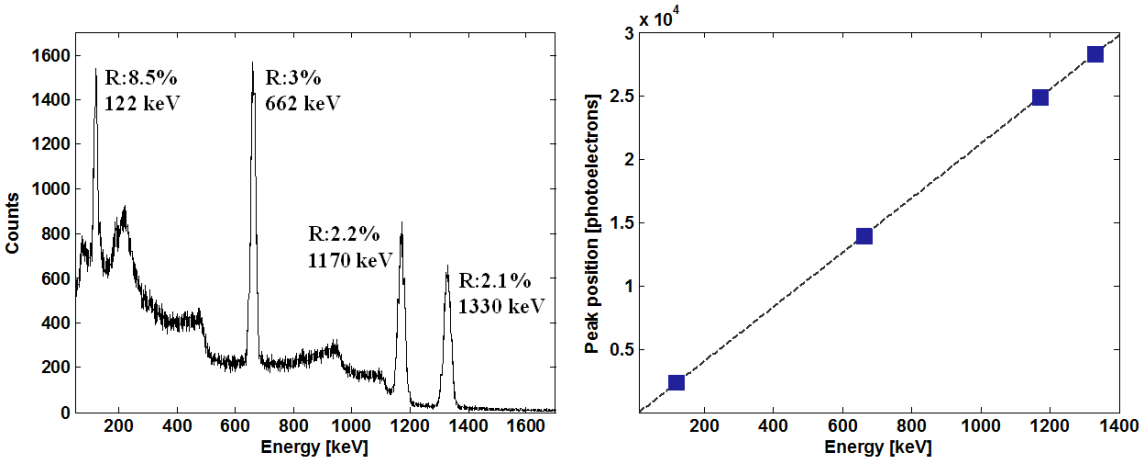

Figure 3. (left) Spectrum acquired with a SDDs matrix coupled to a 1"×1" $LaBr_3$:Ce scintillator and irradiated with three gamma sources (Co-57, Cs-137 and Co-60). The temperature is -20°C and peaking time is 6 μs. (right) Linearity plot of the lines in the spectrum. The maximum deviation from linear fitting is below 0.5%.

3 Gamma-ray spectroscopy with a 1"×1" $LaBr_3$:Ce scintillator

3.1 Experimental setup

The setup is realized with a compact design to allow measurements at -20 ° C with uniform and slow cooling being utilized to minimize risks of damage to the scintillator crystal. The scintillator is positioned on the array by means of a metallic holder, which has the double role to guarantee a precise alignment with respect to the SDDs array and to allow a uniform cooling in the crystal volume. Heat is removed by the holder and by the detector plane by a Peltier stage, placed below the assembly. The whole system is finally enclosed within plastic walls in a dry atmosphere. Thermal simulations have been performed to study and optimize the cooling capability of the system.

3.2 Experimental results

The SDD array was coupled to a 1"×1" $LaBr_3$:Ce scintillator by means of an optical grease (BC-630 - Saint Gobain) and measurements were performed at a temperature of -20°C. The system was irradiated simultaneously with three different sources: Co-57, Cs-137 and Co-60. In figure 3 (left), the energy spectrum measured with 6 μs peaking time is shown, with a 3.0% energy resolution measured at the 662 keV line. For reference, the same scintillator sample, readout with a conventional PMT detector, shows an energy resolution of 3.2% at the same energy (courtesy F. Quarati, Delft University, The Netherlands).

Non-linearity can be evaluated by means of a linear fitting between the measured positions of the peaks in photoelectrons and the nominal energies in keV, as depicted in figure 3 (right). The maximum non-linearity calculated with this method is below 0.5%.

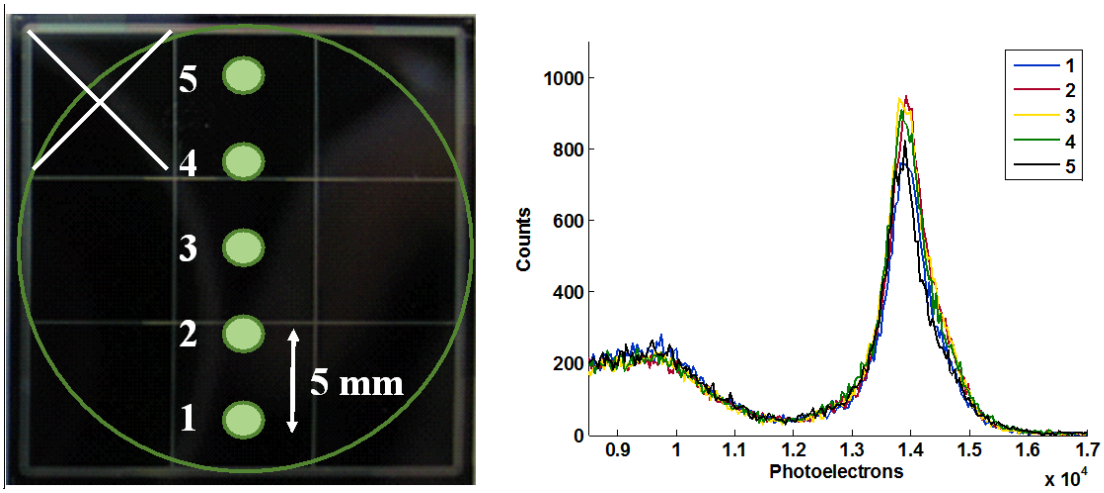

Figure 4. (left) Scheme of the position measurement: the green line is the scintillator, the five circles represent the different points of irradiation. The upper left SDD was not working properly and hence switched off. (right) The spectra of the five irradiation points are well aligned, showing a negligible position-dependence on light collection.

4 Gamma-ray imaging with a 1"×1" $LaBr_3$:Ce scintillator

4.1 Position sensitivity

A position sensitivity of 1–2 cm in large volume $LaBr_3$:Ce scintillators (1"×1" and 3"×3") has already been proved using position sensitive PMTs [4]. In this work, we explore the performance that can be obtained with our SDD-based detector.

The position sensitivity has been evaluated by irradiating the scintillator with a 1 mm collimated Cs-137 source. The collimator with a 1 mm diameter aperture is realized with a mold using a tungsten-based alloy.

The top side of scintillator was scanned with steps of 5 mm along both the horizontal and vertical directions to assess the position sensitivity of the system, i.e. the capability of the array to show different signals on the SDD units related to different positions of interaction of the source. Unfortunately, after placing the scintillator, one SDD on the corner showed an anomalous behavior and hence its corresponding channel was switched off.

Figure 4 (left) refers to the scan along the vertical direction, where the numbers 1 to 5 represent five different irradiation points, with one acquisition of 2 minutes for each p oint. Since the system must perform both spectroscopy and position measurements, it is essential to verify that the measured spectra, determined as the sum of the eight signals of the array, are position-independent, otherwise an undesired broadening in the energy resolution is introduced. Figure 4 (right) shows the five spectra superimposed, with reduced resolution due to the missing channel, whilst no relevant distortion of the 662 keV peak is evident.

The position sensitivity is evaluated in figure 5 (left). The eight sub-plots represent the eight SDDs signals, while the x-axis is related to the five irradiation spots with the notation introduced in figure 4 (left). The y-axis reports the number of photoelectrons measured by the related SDD, calculated as the average value for all the detected gamma-rays events in the 662 keV photopeak

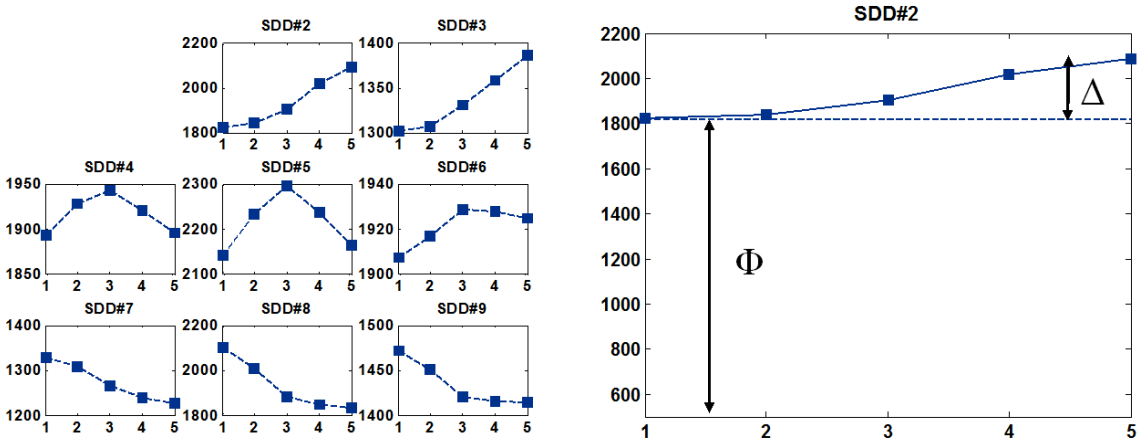

Figure 5. (left) Average distribution of photoelectrons readout by each SDD as a function of the five points of irradiation. (right) The average signal is composed by a predominant baseline (Φ) and a varying contribution (Δ) which contains information about the position of interaction.

energy window. Therefore, the figure shows the average fraction of light readout by each SDD as a function of the point of interaction. Moving the source from the bottom (position 1) to the top part (position 5) of the scintillator, the average signals vary with a coherent behavior. For example, subplot SDD#2 and SDD#8 have an opposite trend: the average number of photoelectrons decreases when the source moves away and increases as it gets closer. On the other hand, subplot SDD#5 reaches its maximum when the source is exactly on the center of the scintillator.

4.2 Imaging capability

In order to retrieve the position of interaction and to represent the acquisitions in a planar image, the data must be thoroughly analyzed. In fact, the reflective wrapping and the ratio 1:1 between thickness and diameter of the scintillator tend to spread light quite uniformly over all photodetector units, with limited dependence from the point of interaction of the gamma event in the crystal. It can be observed in figure 5 (right) that the average signal is composed by a dominant constant component (Φ), a baseline of thousands of photoelectrons spread uniformly over all units, and an additional contribution (Δ), which depends on the position of interaction, of only few hundreds photoelectrons. One possibility to calculate the position of interaction is to use a modified version of the centroid formula [12]:

$$X_C = \frac{\sum (Q_i - \Phi_i)^n x_i}{\sum (Q_i - \Phi_i)^n} \qquad Y_C = \frac{\sum (Q_i - \Phi_i)^n y_i}{\sum (Q_i - \Phi_i)^n}$$

where Q_i is the signal collected by the i-th detector, (x_i, y_i) the coordinates of its center and Φ_i is the baseline value to subtract. In the original formula, Φ is a value equal for all the detectors, but not in our case, in which, e.g. in the four corners, the units are only partially covered by the scintillator and hence they receive less light than the central SDD. The parameter n is usually set empirically with values between 1 and 3. In our case we choose 1.8. Figure 6 shows the reconstruction of five irradiation points distributed on along both x and y axes. In the reconstruction of the corresponding

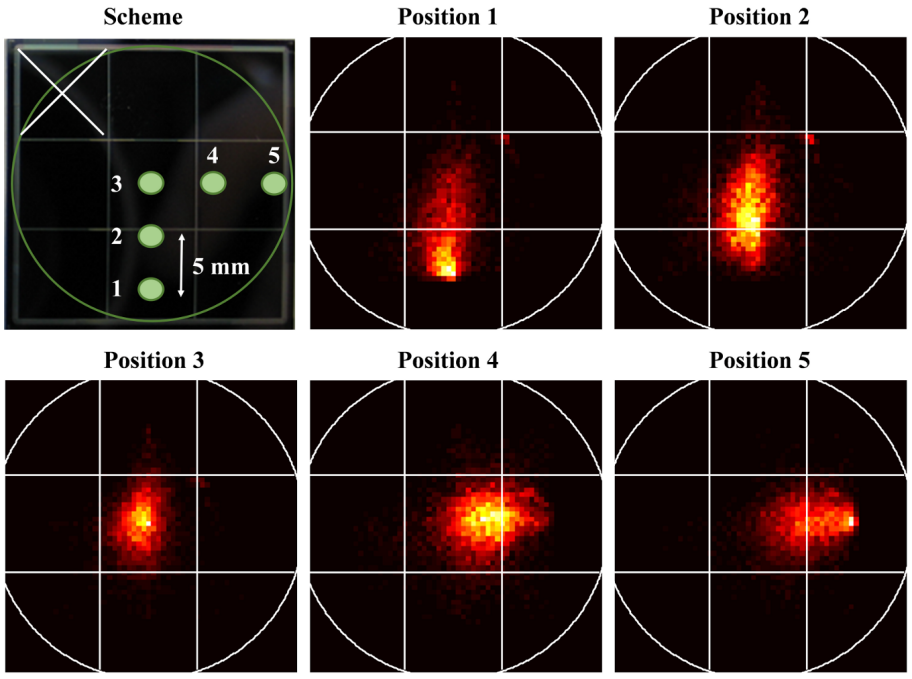

Figure 6. Image reconstruction of five points arranged on a half cross on both x and y coordinates. Even using a simple centroid method, a different position can be observed in the reconstruction of the different points of irradiation. For reference, the squares corresponding to the SDD units (8 mm side each) are also reported in the figure.

measured data with the mentioned algorithm, the system seems to correctly track the change of position of the different irradiation points.

5 Conclusions

In this work we have presented a prototype of a gamma detector based on SDDs coupled to a $LaBr_3$:Ce crystal. The architecture of the camera has been described and the first results are reported. The detection module array coupled to a 1"×1" crystal has shown good results in terms of energy resolution, with a value of 3.0% at 662 keV. Despite the rather inconvenient thickness/diameter ratio of the prototype and the all-reflecting surfaces, the system has also demonstrated position sensitivity using a collimated Cs-137 source and the possibility to reconstruct planar images with a modified version of the centroid method. The development of the final prototype to readout 2"×2" and 3"×3" crystals is now in progress.

Acknowledgments

The authors would like to thank S. Masci for mounting and bonding of the detectors, S. Incorvaia for designing and manufacturing the setup and F. Quarati for providing the 1"×1" $LaBr_3$:Ce scintillator.

References

[1] S. Kraft et al., *Development and characterization of large La-Halide gamma-ray scintillators for future planetary missions*, *IEEE T. Nucl. Sci.* **51** (2007) 873.

[2] F. Quarati, et al., *X-ray and gamma-ray response of a 2"×2" LaBr3:Ce scintillation detector*, *Nucl. Instrum. Meth.* **A 574** (2007) 115.

[3] A. Giaz, et al., *Characterization of large volume 3.5"×8" LaBr3:Ce detectors*, *Nucl. Instrum. Meth.* **A 729** (2013) 910.

[4] F. Birocchi et al., *Position sensitivity of large volume $LaBr_3$:Ce detectors*, *Proc .Nucl. Sci. Symp. Conf.* (2009) 1403.

[5] P. Lechner et al., *Silicon drift detectors for high resolution room temperature X-ray spectroscopy*, *Nucl. Instrum. Meth.* **A 377** (1996) 346.

[6] P. Busca et al., *Silicon drift photo-detector arrays for the HICAM gamma camera*, *Nucl. Instrum. Meth.* **A 624** (2010) 282.

[7] C. Fiorini et al., *Gamma-ray spectroscopy with $LaBr_3$:Ce scintillator readout by a silicon drift detector*, *IEEE T. Nucl. Sci.* **53** (2006) 2392.

[8] C. Fiorini et al., *Silicon drift detectors for readout of scintillators in gamma-ray spectroscopy*, *IEEE T. Nucl. Sci.* **60** (2013) 2923.

[9] C. Fiorini et al. *Single-side biasing of silicon drift detectors with homogeneous light entrance window*, *IEEE T. Nucl. Sci.* **47** (2000) 1691.

[10] L. Bombelli et al., *Low-noise CMOS charge preamplifier for X-ray spectroscopy detectors*, *Proc. Nucl. Sci. Symp. Conf.* (2010) 135.

[11] R. Quaglia et al., *Readout electronics and DAQ system for silicon drift detector arrays in gamma ray spectroscopy applications*, *Proc. Nucl. Sci. Symp. Conf.* (2012) 922.

[12] R. Pani et al., *Investigation of depth dependent response of continuous LaBr3:Ce scintillation crystals*, *Proc. Nucl. Sci. Symp. Conf.* (2009) 3839.